

## Local Approach to Fracture of an Aged Duplex Stainless Steel

Alfredo Hazarabedian<sup>a\*</sup>, Pierre Forget<sup>b</sup>, Bernard Marini<sup>b</sup>

<sup>a</sup> DM/CAC/CNEA Av. del Libertador 8250, (1430) Buenos Aires, Argentine

<sup>b</sup> LEM/SRMA/CEA-SACLAY, France

Received: August 17, 2001; Revised: April 29, 2002

The local approach to fracture (LAF) is a methodology aimed to calculate macroscopic fracture properties of a body, from the knowledge of the local stress - strain field at the fracture site, and the modeling of the acting fracture mechanisms. In the present work, this method was applied to a CF8M steel, aged 30000 h at 325 °C, in order to elucidate if LAF could be able to describe the measured fracture toughness data. We have simulated the elastoplastic behavior using the Gurson model and the general methodology of Joly. The required parameters were obtained from the stress - strain curve and from the damage progression study by quantitative metallography. We extended the validity of that methodology for a material aged in a more realistic condition, i.e. at a relatively lower temperature and for a longer time. The model was found satisfactory because it was able to describe the experimental distribution of the fracture probability vs. fracture strain of notched axisymmetric specimens, without any parameter fitting. The model also predicted the lower bound of the experimental distribution of the crack resistance at 0.2 mm of crack extension ( $J_{0.2}$ ).

**Keywords:** local approach to fracture, toughness, duplex stainless steels, aging

### 1. Introduction

One of the materials used in cast components of nuclear power plants primary circuits is the family of cast corrosion resistant stainless steels ASTM CF3, CF8 and CF8M. They have a duplex microstructure composed of ferrite and austenite. Long time of operation (greater than 10000 h), at hot branch temperatures (approx. 325 °C) or cold branch temperatures (280 °C), cause an aging phenomenon, similar to the 475 °C embrittlement of ferritic stainless steels<sup>1</sup>. Aging hardens ferrite, and consequently the overall hardness and strength increase. However, ductility, toughness and impact resistance decrease, the ductile-brittle transition shifts to higher temperatures and the upper shelf energy is reduced. It is necessary then, in order to assess component life, to determine the amount of mechanical properties degradation, in particular fracture toughness. Aging depends on many factors, the mostly reported are the ferrite content, thermal history, microstructure, chemical composition and texture<sup>2</sup>. Experimental results present a wide scatter that difficult the tasks of predicting a component state from a laboratory study. To face this problem, methods based on the local approach to fracture are used<sup>3</sup>. This model was developed using an accelerated aged (at 400 °C) material.

Damage and fracture mechanisms of aged duplex stain-

less steels are known and are well documented in the literature<sup>4</sup>. Ferrite is hardened by demixing by the precipitation of ordered Cr rich phases or by spinodal decomposition. Hardening promotes strain localization and the premature cracking of ferrite islands. These cracks act as nuclei of the cavities that lead to the final ductile fracture by growth and coalescence. Joly<sup>3</sup> showed that this damage is not uniformly distributed. Some regions are more prone to fracture. These regions have the size of the ferritic packet (approximately 0.5 mm<sup>3</sup>) and belong to regions whose crystallographic orientations favor the cracking process. In particular, packets oriented in such a way that only one slip system is activated are much more damaged than the rest. The size, distribution, and damage rate inside these regions control overall ductility.

Our aim is to implement a method based on the "local approach to fracture" to predict the fracture toughness of this kind of materials. In this approach, material fracture-mechanical properties are estimated from the knowledge and modeling of the acting micromechanisms of damage and fracture and the evaluation of the local stress-strain field.

### 2. Material

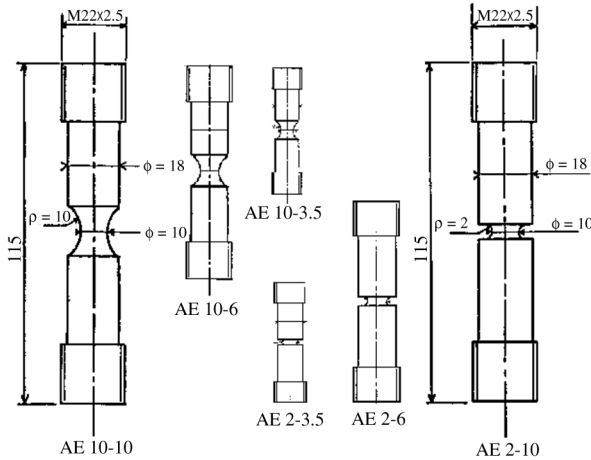
A 32%  $\delta$  ferrite steel, corresponding to an out of specification case was chosen to in order give a conservative pre-

\*e-mail: hazarabe@cnea.gov.ar

Trabalho apresentado no IV Colóquio Latinoamericano de Fractura y Fatiga

**Table 1.** Chemical Composition and ferrite content of material.

Material	C	Cr	Ni	Mo	Mn	Si	N <sub>2</sub> (ppm)	δ
F32	0.033	22.28	9.92	2.34	0.91	0.86	510	32%

**Figure 1.** Notch axisymmetric specimens geometry.

diction of the mechanical properties degradation. This heat was produced using a methodology representative of that applied for the reactors components manufacturing.

### 3. Mechanical Tests

Tensile mechanical properties were measured using a standard 8 mm diameter and 40 mm gage length specimens. To obtain a sample of the fracture probability vs. fracture strain, necessary for the local approach to fracture methodology, tensile tests were carried out on U notched axisymmetric specimens with 10 mm diameter at the notch root. To study the effect of the stress triaxiality on the fracture mechanism, two different notch radius, with 2 mm and 10 mm, were used. In addition, in order to put in evidence the size effect, similar sub-sized specimens at 60% and 35% of the standard size were tested, as shown in Fig. 1.

Fracture toughness was measured following the standard draft P1-87D from EGF<sup>5</sup>, for the ductile fracture. J-Δa curves from three specimens were obtained by the compliance method, and from two specimens using the unique specimen technique. 2-mm side grooved CTJ20 (20 mm de wide) specimens were used in this study.

### 4. The Model

Material was modeled using an elastoplastic porous (Gurson – Tvergaard<sup>6</sup>) constitutive equation:

$$\sigma_{eq}^2(\epsilon_{eq}^p) = \sigma_y^2(\epsilon_{eq}^p) \sqrt{1 - 2f(\epsilon_{eq}^p) q_1 \cosh\left[\frac{3}{2} \frac{\sigma_m(\epsilon_{eq}^p)}{\sigma_y}\right]} \quad (1)$$

where  $q_1$  is a constant, ( $\sigma_m$ ,  $\sigma_y$  and  $\sigma_{eq}$  are the hydrostatic, yield and equivalent stresses respectively,  $\epsilon_{eq}^p$  is the equivalent plastic deformation and  $f$  is the volume fraction of pores (porosity). In the Gurson model, an increase of the porosity lowers the yield stress for a given plastic deformation, compared to a non-damageable material. In ferritic pressure vessel steels, cavities appear at the onset of plastic deformation. Then, the porosity increases only by the growth of the initial cavities. For this reason, in many Gurson model implementations, the cavity nucleation term is neglected. For aged duplex steels, where microcracks nucleate during the plastic deformation, Joly<sup>3</sup> includes the nucleation term, which is proportional to the equivalent plastic deformation. The porosity is modeled like:

$$\frac{df(\epsilon_{eq}^p)}{d\epsilon_{eq}^p} = f q_1 \frac{3}{2} \cosh\left[\frac{3}{2} \frac{\sigma_m}{\sigma_{eq}}\right] + A_n \quad (2)$$

If deformation and damage are assumed uncoupled, this equation can be analytically integrated. Then:

$$f = A_n J \exp(I) \quad (3)$$

where

$$J = \int_0^{\epsilon_{eq}^p} \exp(-I) d\epsilon_{eq}^p \quad \text{and} \quad I = \int_0^{\epsilon_{eq}^p} \frac{3}{2} \sinh\left[\frac{3}{2} \frac{\sigma_m}{\sigma_{eq}}\right] d\epsilon_{eq}^p \quad (4)$$

The unique input parameter for this model, despite the tensile curve, is the *cavity nucleation rate*;  $A_n$ . Following Joly's model, we consider it to be a random parameter, obeying a uniform distribution inside an interval and null outside.

To predict fracture we use the weakest link hypothesis. This means that there exists a characteristic size  $V_0$  or representative volume element (RVE) of a material, which failure leads to the specimen or structure overall fracture. The probability of fracture ( $P_R$ ) of the whole material under the weakest link hypothesis is:

$$V_0 \in V \quad 1 - P_R = \prod_{V_0 \in V} (1 - p_r) \quad (5)$$

where  $p_r$  is the probability of fracture for each RVE. A local criterion for plastic instability can be used in order to evaluate if a RVE fails. Then, this instability will be attained if a critical porosity  $f_c$  (function of the equivalent plastic deformation) is achieved:

$$\frac{d\sigma_{eq}}{d\varepsilon_{eq}^p} = 0 \Leftrightarrow f_c(\varepsilon_{eq}^p) \quad (6)$$

To reach this condition,  $A_n$  must exceed a critical value  $A_{nc}$ , which is a function of the local plastic history (an increase of the plastic deformation will result in a lower value of the critical crack nucleation rate).

$$p_r(V_0) = p(f \geq f_c) = p(A_n \geq A_{nc}) \quad (7)$$

First, the computed RVE must be a crack susceptible site. Then, the probability of fracture of a given RVE will be the product of the probability  $\phi$  that this volume be a crack susceptible site, by the probability that its crack nucleation rate  $A_n$  is greater than the threshold value given by the local stress – strain field:

$$p(A_n \geq A_{nc}) = \phi(RVE \in \text{weak sites}) \cdot \phi(A_n \geq A_{nc}) \quad (8)$$

Probability  $\phi$  and the parameters determining the  $A_n$  distribution were determined in the first part of this work<sup>7</sup>, using a replica technique for the study of crack nucleation. Voronoï analysis allowed to identify and to measure the size, the relative volume fraction of the crack clusters, and the mean nucleation rate of cracks inside them:  $\bar{A}$ . These clusters indicate the weak regions where cracking and porosity develop profusely. It is assumed that  $A_n$  obeys a distribution that is uniform inside the interval  $(0.5\bar{A}, 1.5\bar{A})$  and is zero outside. The volume fraction of weak clusters is assigned to  $\phi$ . This analysis gave the following results:

$$\bar{A} = 0.44; \quad \phi = 0.063 \quad \text{and} \quad V_0 = 42 \times 10^{-3} \text{ mm}^3$$

Probability of fracture was computed post-processing the finite element solution of the elastoplastic undamageable material. Because after the failure of the first RVE the nucleation porosity can not be neglected, that solution does not describe adequately the specimen behavior. For this reason, we can only attempt to predict fracture initiation, not it's propagation. CEA's Finite Element Code *CASTEM 2000*<sup>8</sup> was used for these calculations.

To verify the model and the simulations, numerical results were compared to notched axisymmetric specimen data. If the model describes the distribution of the fracture probability vs. the deformation at fracture of the notch axisymmetric specimens, then it could be applied to predict the behavior of the compact specimens.

## 5. Results

The effect of aging and of the triaxiality on the mean deformation at the notch root is shown in Fig. 2. Aging lowers the values of the deformation at fracture. The width of

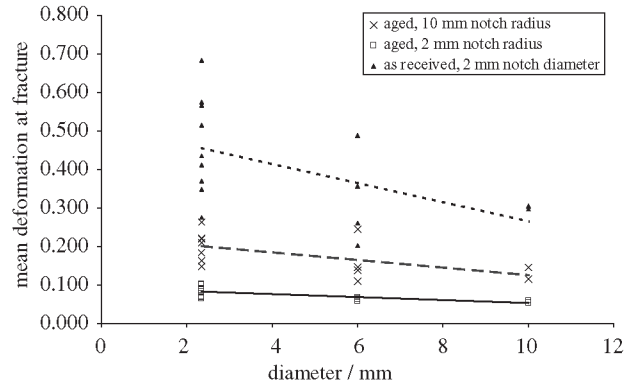


**Figure 2.** Effect of thermal aging and the specimens geometry on the mean deformation at fracture.

the scatter band, relative to the mean value for the each condition is not enlarged after aging. The experimental fracture probability of the each specimen  $P_R(i)$  is calculated as:

$$P_R(i) = (i - 0.5) / N \quad (9)$$

where  $i$  is the rank of the experiment (i.e.,  $i = 1$  for lowest and  $i = N$  for the highest property: deformation of fracture for the notch axisymmetric specimens, and  $J_{02}$  for the compact specimens) and  $N$  is the total number of tests<sup>9</sup>.

In order to check the model, the calculated failure probability can be compared to this experimentally determined probability. Using the size effect, the fracture probability of geometrically similar specimens can be compiled into a single curve, in this case to the 35% size. If  $P_1$  and  $P_2$  are the fracture probability of geometrically similar specimens of  $r_1$  and  $r_2$  radius, respectively and under the weakest link hypothesis; these probabilities are related by<sup>10</sup>:

$$r_1 \ln(1 - P_2)^{1/5} = r_2 \ln(1 - P_1)^{1/5} \quad (10)$$

As it could be seen in Fig. 3, the model predicts the probability of fracture of these specimens.

The second step is to evaluate a fracture mechanical property, using the same method. The specimen was simulated using a 2D, plane strain calculation. Here, the failure probability of the element in front of the crack gives the probability of the onset of crack propagation. The result is shown in Fig. 4.

While our simulation can't fit the whole experimental distribution, it predicts that the threshold crack mouth opening displacement (CMOD) for a non-null probability for crack propagation is 0.45 mm.

The  $J_{02}$  value was calculated using the simulated curve and the procedure of the test standard. The value of  $J_{02}$  for CMOD equal to 0.45 mm is 42 kJ m<sup>-2</sup> which falls inside the scatter band of the experimental data for F32 steel's  $J_{02}$

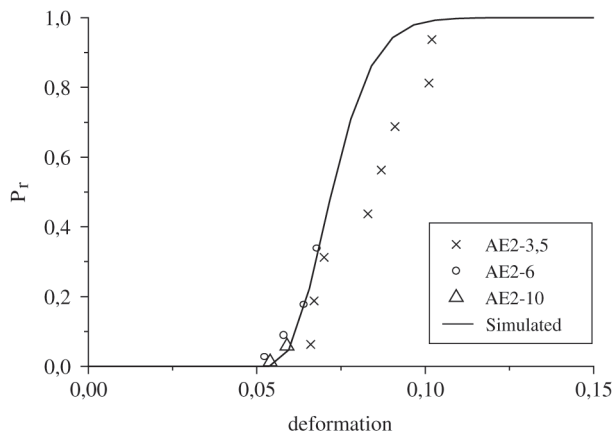


**Figure 3.** F32-T1: Probability of fracture vs. rupture deformation at the middle section of 2 mm notch specimens, normal and sub-size specimens.

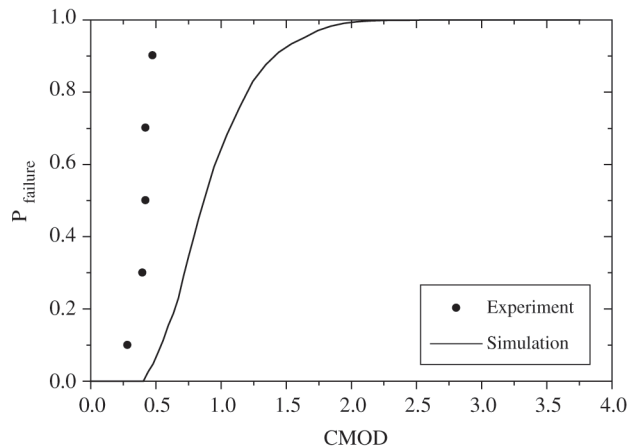


**Figure 4.** F32-T1: Experimental and simulated probabilities of crack growth initiation as function of crack mouth opening displacement (CMOD).

showed in Fig. 5.

## 6. Conclusions

We showed that the Gurson model for an elastoplastic porous material with a cavity nucleation rate proportional to the plastic deformation as proposed by Joly, and using the parameters we obtained from quantitative metallography, describes acceptably, and without any parameter fitting the distribution of the probability of fracture of notched axisymmetric specimens. Then, the extended applicability of the Joly's approach to low temperature – long term aged material was demonstrated. The model also predicts the lower bound of  $J_{02}$  equal to 42 J from our measurements.

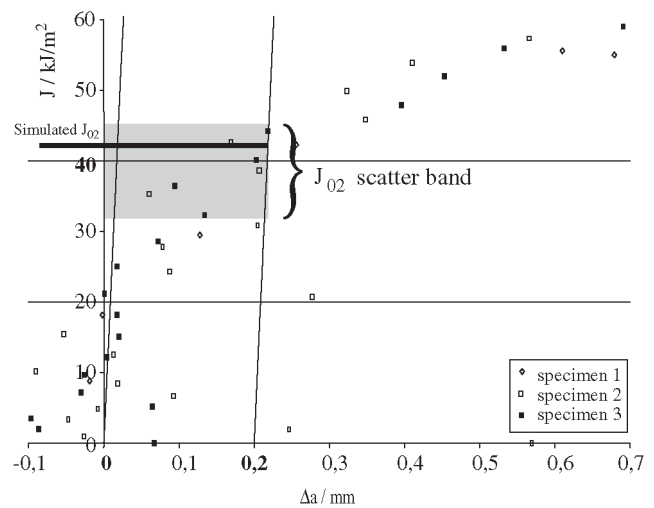


**Figure 5.** F32-T1: Calculated value for the  $J_{02}$  as compared to the experimental  $J$ - $\Delta a$  curve (CTJ20 specimen).

This model slightly overestimates the scatter of the data for the  $J_{02}$ .

## Acknowledgments

This work was part of the firsts author' stay at the "Laboratoire des Études Mécaniques" of Commissariat à l'Énergie Atomique, DEN/DMN/SRMA – Gif-sur-Yvette, 91191 - France, in the course of IAEA - CEA - CNEA. ARG/83 cooperation contract.

## References

1. Slama, G.; Petrequin, P.; Mager, T. "Effect of aging on mechanical properties of austenitic stainless steel castings and welds", presented in *SMIRT Post-Conference Seminar*, 1983.
2. Chung H.M. "Thermal aging of decommissioned reactor cast stainless steel components and methodology for life prediction". *PVP*, ASME, v. 171, p. 111-125, 1989.
3. Joly, P. Doctoral Thesis "Étude de la rupture d'aciers inoxydables austéno-ferritiques moulés, fragilisés par vieillissement à 400° C" École des Mines de Paris. May 1982.
4. Chung H.M. "Aging and life prediction of cast stainless steel components". *Intl J. Press. Vessel & Piping*, v. 50, p. 179-213, 1992.
5. Schwalbe, -K.H.; Neale, B.K.; Ingham, T. "Draft EGF recommendations for determining the fracture resistance of ductile materials: EGF procedure EGF P1-87D". *Fatigue Fract. Eng. Mater. Struct.*, v. 11, n. 6, p. 409-420, 1988.
6. Gurson, A.L. "Continuum theory of ductile rupture by void nucleation and growth: Par 1 - Yield criteria and

- flow rules for porous ductile media”, *J. of Eng. Mat & Tech.*, v. 99, p. 2-15, 1997.
- Tvergaard, V. “On localization in ductile materials containing spherical voids”. *Intl. J. of Fracture*, v. 18, p. 237-252, 1982.
7. Hazarabedian, A.; Marini, B. “Quantification of damage progression in a thermally aged dual Stainless Steel”, *Mat. Res.*, v. 5, n. 2, p. 113-117, 2002.
8. Verpeaux, P.; Millard, A.; Hoffmann, A.; Ebersolt, L. “Castem 2000: a modern approach of computerized structural analysis”. *Seminar on recent advances in design procedures for high temperature plant*. Risley. UK. 8-9 Nov 1988.
9. Wiesner, C.S.; “The ‘Local Approach to Cleavage Fracture’”. Appendix C. Abington, Cambridge. (1996).
10. Marini B. “Rupture des aciers et effets d’échelle” *J. De Physique. IV proceedings*, v. 8, p. Pr4-95 - Pr4-104, 1998.